Numerical modelling and CFD simulation of a polymer electrolyte membrane (PEM) fuel cell flow channel using an open pore cellular foam material

Awotwe, Tabbi; Khatib, F.N.; Ijaodola, O.S.; Ogungbemi, E.; El-Hassan, Zaki; Durrant, A.; Thompson, J.; Olabi, A.G.

Published in:
Science of the Total Environment

DOI:
10.1016/j.scitotenv.2019.03.430

Published: 15/08/2019

Document Version
Peer reviewed version

Science of the total environment
ARTICLE

Numerical Modelling and CFD Simulation of a Polymer Electrolyte Membrane (PEM) Fuel Cell Flow Channel Using an Open Pore Cellular Foam Material

Tabbi Wilberforce[1] , F. N. Khatib[*1], O. S. Ijaodola[1], E. Ogungbemi[1], Zaki El - Hassan[1], A. Durrant[1], J. Thompson[1], A. G. Olabi[2,3]

1. Institute of Engineering and Energy Technologies, University of the West of Scotland, PA1 2BE, UK
2. Dept. of Sustainable and Renewable Energy Engineering, University of Sharjah, P.O. Box 27272, Sharjah, UAE
3. Mechanical Engineering and Design, Aston University, School of Engineering and Applied Science, Aston Triangle, Birmingham, B4 7ET, UK

ABSTRACT

Fuel cell performances varies with different structural configurations and materials. However, the two main areas that determine this performance metric are the membrane electrode assembly (MEA) and the bipolar plates. The MEA provides the platform for the electrochemical reaction to occur and the bipolar plate serves as a medium between the reactants (hydrogen and air) and the catalyst layer. The bipolar plate is the first point of contact for the reactants inside the fuel cell, so a badly designed item with a high pressure drop will have a negative impact on fuel cell performance. Numerical modelling and simulation tools like ANSYS have a huge impact on engineering industry as they help designs to be validated and analysed before any physical construction.

This investigation considers five suitable flow plate designs for PEM fuel cell, each completely different from the readily available, traditional serpentine designs on the market. The work explored the possibility of replacing these flow channels with an aluminium cellular foam with different inlet and outlet orientations. The designs were further optimised and modelled in ANSYS.

The results obtained were compared with other designs in the literature. Compared to the serpentine flow design, the open pore cellular foam material showed a very small pressure drop in the range of 30-40 Pa. This indicates a possibility of replacing the traditional flow plate designs with the proposed ones.

Key words: Computational Fluid Dynamics (CFD), Optimization, Fuel cell, Serpentine, Design of Experiment (DOE)

INTRODUCTION

Fuel cells are electrochemical devices that transform the chemical energy of reactants into electrical energy with a very high efficiency. Fuel cells produce waste heat and generate water as a reaction product. The fuel (hydrogen) is supplied to the negative electrode (anode) while the oxygen from air being the oxidant is supplied to the positive electrode (cathode) as seen in Proton Exchange Membrane fuel cells, among others. The chemical reaction at the anode produces electrons for an electric current. All fuel cells have very high efficiencies which are often independent on the size of the system. Their design is also scalable and they produce zero or almost zero greenhouse gas emissions. As they have no moving parts, their operation is highly reliable as a result of their being vibration-free and less susceptible to wear and tear [1]. Fig. 1 shows a 3D view of a five stack fuel cell.

Though the advantages of fuel cells are enormous, their disadvantages cannot be overlooked. Cost remains a major challenge to the fuel cell industry, which has impaired their commercial success for general use. Storage of pure hydrogen is also a major issue. In situations where fuel that is not pure is used, additional fuel reformation technology has to be taken into account. Fuel cell performance also decreases when impure hydrogen gas is used. Traditional power generation

largely depends on fossil fuels which are now being discouraged around the world because of their high impact on the environment. Fuel cells are used for a number of portable applications, in the transportation sector and even the stationary sector. Most scientists believe that portable devices like mobile telephones and laptop computers will soon demand high power to keep them running for longer. As fuel cells are scalable with very simple recharging capabilities compared to batteries, they are a suitable option for portable devices in the near future. The limitations of fossil fuels and the high demand for them by the transport industry contribute to fluctuations in prices, necessitating an alternative energy source. In its defence, the transport industry has undergone significant recent improvement as there is a growing number of hydrogen fuel cell cars on today's roads, with researchers still conducting investigations to improve the current automobile technology to develop a product that is cheaper and more reliable. The unreliability of the power supply in some parts of the world affects most companies negatively [2]; an improvement in current fuel cell technology will do much to alleviate this. In order to generate more electricity and heat for living space, the stationary fuel cell is usually preferred. There are currently eight types of fuel cells available: Alkaline Fuel cells (AFCs), Phosphorous Acid Fuel cell (PAFCs), Solid Oxide Fuel Cells (SOFCs), Molten Carbonate Fuel cells (MCFCs), Zinc-air fuel cells (ZAFCs), Protonic Ceramic Fuel cells (PCFCs), Biological fuel cells (BFCs) and Proton Exchange Membrane fuel cell (PEMFCs)[2,3]. The PEMFC, also called the polymer electrolyte cell, generates a high power density at low weight, cost, and volume. PEMFCs are normally made up of an anode, cathode and an electrolyte membrane as shown in Fig. 2.

Oxidation of hydrogen occurs at the anode while reduction of oxygen occurs at the cathode. The electrons are transported from one to the other through an electric circuit, hence the fuel cell is used as a DC source. The fuel cell has a carbon paper, mainly for covering the electrolyte on both

anode and cathode sides of the fuel cell. The porosity of this backing layer is normally in the range 0.3 to 0.8. It plays a vital role in the transfer of the reactants as well as the reaction product to the flow plate of the reactive sites [3]. While the electrons produced at the anode are drawn away into the electric circuit, the ions that also result from the electrochemical reaction travel through the electrolyte to cathode. At the cathode, an electrochemical reduction occurs due to the electrons returning from the external load. One actively used electrolyte material, Fluorinated Teflon by Dupont, is mostly used in PEM fuel cells and referred to as a "Nafion membrane", as shown in Fig. 3.

Nafion membranes provide a high chemical reaction and thermal stability. The electrodes are thin films that are well attached to the membrane. Electrodes with a low platinum loading perform well compared to those with a high platinum loading. Adding the polymer in a soluble state into the pores of the support structure (carbon) is one of the approaches taken to improve the usage of the platinum. The interface between the electrocatalyst and solid polymer electrolyte is increased by adapting this approach. Water management in the fuel cell is very crucial, as less or more water could damage the fuel cell. Therefore fuel cell design must carefully consider flooding and its prevention. The electrochemical reaction produces water which is expected to leave the cell after the electrochemical process but poor cell design means it is produced faster than its rate of escape.. This flooding prevents the MEA from functioning at its full potential hence nearly one-third of the MEA surface is utilised. [4-6]. The bipolar plates and the membrane electrode assembly are the two most important parts of the fuel cell. The transport of the reactants to the reactive site occurs through the bipolar plate. The membrane electrode assembly, having the platinum catalyst layer on its surface, functions as the platform where the electrochemical reaction occurs. Supplying reactant at high concentrations to the catalyst layer with less obstruction will therefore significantly

improve fuel cell performance. The design of the bipolar plate is also important as it determines the water management through the cell and creates a platform where the generated current can be collected [7]. The membrane electrode assembly is often located between two flow plates. It is composed of a proton exchange membrane and a gas diffusion layer which is porous in nature but conductive electrically. Bipolar plates in the fuel cell are normally made of graphite with a metallic housing but this design is gradually falling out of practice. Most newly developed PEM fuel cells are made of a polymer called acetyl to reduce the weight of the fuel cell, which in effect reduces its overall cost [8-10]. Fig. 4 shows some new types of fuel cell on the market that use acetyl.

Though graphite has some good electrical properties, it has some major setbacks that have prompted the paradigm shift by researchers around the world from relying on it as the sole material for the bipolar plate. The tensile strength of graphite is very low and it is also very brittle. It is also very expensive to machine. With the bipolar plate accounting for almost 70% of the weight of the entire cell according to Lawlor et 2009, Dong *et al.*, 2007 [11, 12], it is recommended that the material for the bipolar plate be made lighter as nearly 40% of the cost of a fuel cell depends on the bipolar plate.

Metals have recently become more popular as the material of choice for bipolar plates as their advantages include low cost, ease of processing, high mechanical strength, high electrical conductivity and high thermal conductivity. The normal practice is for the flow channels to be machined on the bipolar plate. This is done to achieve uniform distribution of the reactants and thus helps make better use of the MEA. The flow channel can be straight, parallel and even serpentine [11 – 15]. Other investigations concluded that the performance of any fuel cell is highly dependent on the bipolar design [13 – 20]. This is simply because a poorly designed bipolar plate, as mentioned earlier, often leads to problems with water removal and obstructs reactant transport.

Another researcher undertook a detailed study of the various types of flow plates in a fuel cell and also recommended that, for effective fuel distribution, the bipolar plate must be carefully designed [21]. It therefore confirms that an improperly designed bipolar plate will lead to uneven distribution of the electrochemical reactant in the fuel cell, which reduces the utilisation of the catalyst layer [22]. Open pore cellular foam (OPCF) material has recently been used by a number of researchers around the world as an alternative to the traditional flow field design. This is simply because the gas distribution through the OPCF material is fairly even, overcoming the poor distribution in other set-ups. Again, the pressure drop between the inlet and outlet through the open pore cellular foam material (OPCFM) is subject to the size of the pores of the foam [23 – 25]. Fig. 5 shows an OPCFM with a porosity of 90% obtained from Goodfellow, UK.

Carbon foam has been utilised as the gas flow field was first proposed by Marice *et al.* [26]. Other researchers, like Tsai *et al/* [27], also confirmed that flow plate material made of metal foam contributed significantly to the efficiency of the fuel cell. They critically explored the effect that flow plate design had on the efficiency of PEM fuel cells. Their investigation brought to light that flow plate designs play an active role when building a fuel cell using foam material or even the traditional fuel cell designs. Kumar and Reddy [28, 29] used foam material in place of channels of conventional flow plates. This modification is not considered appropriate as the full benefit of the OPCFM was not explored. With all these advantages of using the OPCF, researchers are still facing challenges in relation to the housing unit where the foam will be placed. The present work is an extension to earlier work [2] where in this investigation a newer approach to the designs have been carried to optimise the use of Open Pore cellular foam materials. This paper seeks to investigate a new housing unit for the OPCF material, where the results are analysed on the pressure, flow regimes and velocity profiles.

There has been a big increase in the precision of engineering designs as scientists are better able to predict the success or failure of their designs by simulation, thus saving time and money Computational fluid dynamics (CFD) simulation software is one such example, as it can predict and analyse the various flow regimes in a fuel cell design and, in some cases, compute the stresses as well. Research into the development and optimisation of flow plates has been studied using CFD simulations [30-37]. Apart from many uses, CFD is also capable of providing information about the distribution of pressure through the flow channel, the pattern of the pressure and the drop in pressure. The velocity at which material enters and leaves the PEM fuel cell can all be predicted using the CFD tool. With this information obtained from the CFD simulation, designers can easily create or modify their designs without wasting energy in the workshop on ideas that are not feasible or practical. One of the important factors considered in a fuel cell is the even distribution of the oxidant (air/oxygen) and fuel (hydrogen) on the Gas diffusion layer. The pressure of these reactants must be distributed evenly over the Gas Diffusion Layer. This is very important as it determines the amount of catalyst being utilised during the electrochemical process. These are the parameters that define fuel cell performance. The flow channels on the bipolar plates serve as the medium to supply and uniformly distribute the oxidant and fuel to the catalyst layer. CFD analysis to help predict the flow distribution across the channels and check the pressure and velocity through the bipolar plate channels was performed by Kumar and Reddy, 2003, [33], Lozano *et al.*, 2008 [36] and Barreras *et al.* 2011 [37]. This research work intends to explore other suitable flow plate designs using OPCF material. The designs were optimised and varied across selected velocities in literature (1, 3, 6, 9, 12 m/s). Different types of manifold designs were considered and their flow regimes were checked through CFD simulation analysis.

NUMERICAL MODELLING, OPTIMISATION AND SIMULATION

As explained earlier, pressure distribution on the gas diffusion layer and the membrane electrode assembly are important parameters when designing a fuel cell. Other factors, like temperature distribution and even the speed at which the reactive gases travel to the reactive site are all very important as they influence the output or efficiency of the cell. The outcome of the simulation can also clearly show areas in the design where there could be the possibility of dead zones. Dead zones are areas around the fluid domain where the gas is static. It could also be described as the area around the fluid domain that may not be in contact with the reactive gas. This leads to accumulation and retention of water in the cell. A vital function of the gas is to be able to carry any water along the channels as it flows towards the outlet of the channel. Accumulation of water prevents some areas on the MEA from being utilised, hence reduces fuel cell performance. Excessive water in the fuel cell could cause flooding of the cell which will also create serious problems in the functionality of the PEM fuel cell. This clearly stipulates that the design of bipolar plate even affect the water management in the cell.

FUEL CELL DESIGN

ANSYS software was used to determine the flow regimes for the bipolar plate of a fuel cell with an active reaction area of 25 cm^2. A number of designs were suggested for the bipolar plate to aid in the channelling of hydrogen to the reactive sites of the MEA. Manifolds were created in order to channel the hydrogen towards the foam material. CFX in ANSYS was used as the CFD technique to analyse housing designs for both the anode and cathode regions of the fuel cell. The electrochemical reaction in a PEM Fuel cell operates under moderate conditions when compared to the other types of fuel cell. The rate at which the various reactive gases travel through the bipolar flow plate design may be low but the fuel cell will still produce some current. Theoretically, it is possible to calculate the pressure drop in the fluid domain but the type of flow must first be

186 determined. The flow could be laminar or turbulent. This is determined through the calculation of
187 the Reynolds number. For the purpose of this investigation, the flow was considered laminar since
188 it has been well established that the reactants inside the fuel cell are in laminar flow, with a
189 Reynolds number Re < 2300. The flow was also kept as a single phase. The laminar flow design
190 was also utilized by Ramos – Alvarado *et al.* [38]. Various designs were then simulated with
191 specific boundary conditions clearly depicted in Table 1. The final model contained 290,000 –
192 316,853 elements. Fig. 6 shows the anode housing designs with their respective CFD mesh using
193 ANSYS CFX.

194 Table 1: Boundary conditions used in running the simulations.

Parameter	**Response**
Design Modeller	CFX
Mesh	Mixed Tet and Quad
Sizing	Proximity and Curvature
Smoothing	Fine
Transition	Fast
Elements	316,853
Solver	CFX
Model flow	Laminar
Fluid	Hydrogen
Solid walls	Aluminum
Porosity	0.93

Inlet Velocity	1m/s
Temperature	320
Monitors	Mass flow Continuity
Interfacial area density	0.50
Heat transfer coefficient	0.01
iteration	100
Solver type	Pressure based – Double precision

From Table 1, the meshing was kept as Mixed Tet and Quad and a fine mesh was generated. The number of elements was also 316,853. The fluid domain for the gas was kept as being porous and the porosity of the aluminium foam used was 0.93. The speed of the gas entering the fuel cell was also maintained at 1 m/s and the flow kept as laminar. The number of iterations was also kept at 100 for convergence to occur during the simulation. The sizing of the mesh was also maintained at proximity and curvature but during the simulation for design 5, which is the serpentine flow channel, the fluid domain was maintained in settings since the channel was not porous.

NUMERICAL MODEL

Extensive research in the design of metal foams have been undertaken, where key characteristics that determine the performance of the foam has been established both experimentally and theoretically [38-45]. One of the performances measured is the pressure drop in the foam material and different mathematical models have been developed. Flow in a porous media can be determined by the well known Darcy's Law [45]:

$\Delta P \quad v$
10

213213 $\frac{}{L} = (\_) V$ (1)

214214

215 Where, ΔP is the pressure drop over length L (m), v is the fluid viscosity (m^2/s), V is the fluid
216 velocity (m/s) and γ (m^2) describes the permeability of a porous media. However, Darcy's law can
217 be used only for low Reynolds numbers (Re < 0.1). In instances where there are high flow
218 velocities (>0.1 m/s), the drag induced by the ligaments of the foam material becomes important.
219 There is also a major influence of both turbulence and inertia and the pressure drop therefore
220 displays a parabolic trend with the increasing velocity [46]. Therefore to consider this, a modified
221 form of D'Arcy model, that describes the pressure drop in the porous medium at these velocities
222 also known as the Hazen Dupuit-Darcy model is used,

223223

224 $$\frac{\Delta P}{L} = \frac{v}{\gamma} V + \rho C V^2 \qquad (2)$$

225

226 Where, ρ is the density of the gas in the medium (kg/m^3), and, $C = f/\sqrt{\gamma}$ is the coefficient related
227 to the structure of the permeable medium, with f being the coefficient of inertia. The permeability
228 γ (m^2) of porous media is related to the porosity and the mean pore radius, is given by [38],

229229

230230 $$\gamma = \frac{\zeta^3}{180(1-\zeta)^2} d_p{}^2 \qquad (3)$$

231231

232 Where, ζ is the porosity of the foam material and d_p is the pore diameter. For the traditional hollow
233 (serpentine) channels, since the flow is laminar in a functional PEMFC, one can define
234 permeability, γ for the channel through the well-known Hagen–Poiseuille equation [38],

$$\gamma = H\frac{{d_h}^2}{32} \quad (4)$$

Where, H = 2.59 (m) is the shape factor which is typical for laminar flows [38], d_h is the hydraulic diameter of the channel (m).

Another mathematical model, by Ergun *et al.* determines the pressure drop in the foam material with spherical particles of diameter d_p. The Ergun equation is commonly utilized where the flow is through a dense bed, however, to draw a comparison between different mathematical models, this equation was also used.

$$\frac{\Delta}{L} = AV + B\rho V^2 \quad (5)$$

Where,

$$A = \frac{150(1-\zeta)}{\zeta^3 {d_p}^2} \quad (6)$$

$$B = \frac{1.75(1-\zeta)}{\zeta^3 d_p} \quad (7)$$

Research in the design and fabrication of metal foams with different manufacturing techniques has also been undertaken [47], where Ashby *et al.* mathematically define the pressure drop in the metal foams as,

$$\frac{\Delta P}{L} = \varepsilon\left(\frac{1}{d_p}\right)\left[\frac{v^m\rho}{\overline{(1-\alpha)^{2-m}}}\right] V^{2-m} {d_L}^{-m} \quad (8)$$

252252

Where, α is the absorption coefficient, d_L is the foam ligament diameter, ε and m are determined experimentally [47]. This equation is in the context of drop the in pressure with respect to transfer of heat, but for the purposes of correlating models, this equation was also used. The effect of the drag and friction due to flow in the foam material was explicitly described by Fourie and Du Plessis [48], where they make use of the tortuosity of the ligament structure, and thus determining the pressure drop as,

$$\frac{\Delta P}{L} = (3-\tau)(\tau-1)\left(\frac{\rho\tau^2V^2}{\zeta^3 d_p}\right)\left(\frac{3C_{dv}}{2}+\frac{C_{df}}{4}\right)\zeta \tag{9}$$

Where,

$$C_{dv} = \frac{24v\zeta}{\rho(3-\tau)d_pV} \tag{10}$$

$$C_{df} = 1 + 10\left(\frac{\rho V^2 d_p(\tau-1)}{2v\zeta}\right)^{-0.667} \tag{11}$$

Where, τ is the tortuosity, C_{dv} and C_{df} are drag and frictional coefficient.

Since the pressure drop in the channel is directly related to the pressure gradient and the channel permeability, the pumping power consumption can be approximated by the product of the pressure drop along the channel and channel flow rate [38]. Wang, 2005 establishes a pumping power parameter as a ratio of the pumping power for the cathode flow (the major part) of the electric power produced by a fuel cell. Unlike an equation that describes the fuel cell polarisation curve, a linear approximation is assumed to be a very good fit for practical operating conditions [38]. Here a modified form of the equation has been established to define a linearisation of a polarisation

curve,

$$V_{cel} = V_o - V_n \quad (12)$$

Where, V_o is the intercept of the polarisation curve, as the actual open circuit voltage is always higher, in the analysis, it has been maintained at 0.9 V. V_n is defined as the linear voltage drop as in equation (13).

$$V = \frac{A_m v \rho L I}{16 \beta_{pump} A_c} \left(\frac{\xi_c}{F C_{O_2}}\right)^2 \frac{1}{\gamma^n} \quad (13)$$

Where, A_m and A_c is the area of membrane and cathode respectively (m^2), v is the kinematic viscosity (m^3/s), ρ is the density (kg/m^3), L is the length (m), I is the current density (A/m^2), ξ_c is the stoichiometric flow ratio, F is the Faraday constant (A/mol), C_{O_2} is the concentration of oxygen (mol/m^3), β_{pump} is the pumping power ratio [38].

RESULTS AND DISCUSSION

One of the simplest means of analysing and optimising flow field configuration is through observation of the distribution of pressure and velocity in the fluid domain. As stated earlier, the selected design must be able to uniformly distribute pressure over the gas diffusion layer at a constant rate. The drop in pressure between the inlet and outlet of the flow channel must be less as well in order for the gas to reach the reactive site early for electrochemical reaction to occur.

DESIGN 1 OF FLOW CHANNEL (D1)

The first observation is the collision of the fluid with the foam as it flows from the inlet. This causes the speed at which the gas is travelling to increase but the obstruction causes a change in direction around the manifold. Convective flow is created along the porous domain. The D1 profile for the distribution of pressure and velocity is shown in Fig. 7. The purpose of this design was to

uniformly distribute the reactant gases over the open pore cellular foam material (OPCFM). The inlet of the design was created to have an obstruction that was oval in shape. This was done so that the gas builds up momentum as it flows around the oval impediment. The downstream part of the flow plate had same features as the upstream. Convective flows are observed as the gas leaves the impediment into the porous fluid domain. From the pressure profile in Fig. 7(a), the pressure of the gas entering the fluid domain is at 3.2 Pa. It reduces as the gas exit the fluid domain at 1.0 Pa, indicating an overall pressure drop of 2.1 Pa. The mass transport which is linked to the efficiency of the fuel cell will also be seriously affected. A uniform pressure and velocity distribution are observed, as shown in Fig. 7(a) and 7(b). The greater portion of the gas will flow through the foam, meaning that the GDL, which will be in contact to the MEA, will have most of its surface in contact with the gas. Hence the release of electrons through the electrochemical reaction will be very high thereby increasing the amount of energy produced. Water found in the pores or channels will be carried to the outlet easily since large areas of the design will have gas flowing through them. This design will, therefore, be suitable for water management in the fuel cell and also the fewer dead zones show the lesser possibility of water accumulation which affects the fuel cell negatively [40].

309309

DESIGN 2 OF FLOW CHANNEL (D2)

The D2 design can be seen in Fig. 8. It consists of an obstruction which is perpendicular to the main inlet but the dimensions for each of the five(5) rectangular impediments are irregular. The design is similar to D1, with the downstream section of the fluid domain same as the upstream. The orientation of the inlet and outlet are diagonal to each other. The pressure distribution according to the pressure profile in Fig. 8(a) shows that D2 has the pressure of the fluid being high at the inlet but reduced at the outlet where the gas exits the fuel cell. From the profile, the mid

region of the design will have the pressure uniformly distributed. In comparison with D1, the inlet pressure for the D2 is lower. There is, therefore, the pressure drop between the inlet region and the outlet of the cell. The efficiency of the fuel cell will be greatly affected due to the effect on mass transport. Greater portions of the MEA will be utilised as the gas will travel through larger portions of D2 compared to that of D1. The outlet velocity for D2 shown in Fig. 8(b) is higher than that of D1, hence any water in the fluid domain or channel will leave the D2 faster than it will D1. There are some regions in the fluid domain of D2 that are low, which , creates dead zones and hence more water accumulated in the fuel cell. It remains one of the major setbacks for this design. The inlet and outlet orientation are also diagonal to each other.

DESIGN 3 OF FLOW CHANNEL (D3)

The D3 design, as shown in Fig. 9, has the orientation of the inlet and outlet being diagonal. The design comes with impediments at the inlet and outlet region of the cell. These obstructions are designed to be both diagonal and perpendicular to the inlet and outlet. It allows the gas to flow to the other parts of the fluid domain but from the pressure profile shown in Fig. 9(a), there is pressure drop from the inlet to the outlet. This drop in pressure is fairly low when compared to those of D1 and D2. From Fig. 9(b), a uniform velocity distribution is observed through the bipolar plate. The general design of D3 will have a negative impact on the efficiency of the PEM fuel cell. This occurs because of the orientation of the inlet and outlet of the fuel cell. The impediment for this design does not allow the fluid to flow through the entire surface of the fluid domain hence not all the surface of the MEA will be utilised. Dead zones will however be created since the gas is unable to flow through every portion of the fluid domain. It indicates that only one-third of the MEA surface may be utilised hence fuel cell performance will be low.

DESIGN 4 OF FLOW CHANNEL (D4)

The D4 design as shown in Fig.10, has the inlet and outlet of the design being symmetrically aligned to the mid portion of the design. From the design shown in Fig. 10(a), the gas travels through each symmetrical section of the fluid domain due to the double impediment at the inlet region on both the left and right side of the design. The obstruction is actually found at the edges of the fluid domain. The gas travels freely from the inlet to the outlet with no impediment at the middle section of the fluid domain. The pressure drop from the inlet region to the outlet region of D4 is low, hence it will have a positive effect on the mass transport of the fluid flowing through the domain. The efficiency will therefore be fairly better compared to the designs discussed earlier. From the velocity profile in Fig. 10(b), there is a lower velocity at the inlet when compared with other designs. There is also less or minimal restriction as the gas flow directly from the inlet to the outlet. This is noticed around the mid-section of the fluid domain. It is also observed that the entire MEA surface would not be utilised. The blue regions in the D4 are also high hence there would be more water accumulation of water which will affect the fuel cell performance.

DESIGN 5 OF FLOW CHANNEL (D5) (SERPENTINE FLOW PLATE)

The D5 design, as shown in Fig. 11, allows gas to travel through a greater portion of the MEA hence it is the popularly preferred flow plate design for most PEM fuel cells. The results from the simulation performed as shown in Fig. 11 exhibited high pressure at the inlet for the first bipolar plate flow channel. As the gas flows through the rest of the channels, it drops gradually in terms of pressure, which means that there would be high-pressure drop on the MEA. The implication is that the mass transport will be affected and effectively lead to a reduction in fuel cell performance. The velocity profile is shown in Fig. 11(b). It clearly shows that the velocity at which the gas travels will be distributed evenly across the whole flow plate design. Due to the nature of the serpentine design, it is able to carry all water in the channel to the outlet hence very effective in

mitigating issues relating to flooding . The velocities of some of the layers at the boundaries are observed to be low particularly around the edges. Annular flows are therefore created as the water is moved to the channel walls. The area marked blue shows the part of the fluid domain where there dead zones could accumulate. Dead zones as defined earlier are sections on the fluid domain where the gas may not travel through due to the design of the flow plate.

VALIDATION OF RESULTS

Some specific velocities used in literature (1, 3, 6, 9, 12 m/s) [9] were integrated into ANSYS. The simulation was carried out to give a detailed idea of various situations that may occur in the fluid domain as the gas moved from the inlet to the outlet. It therefore showed the drop in pressure for each design as the gas travelled through the fluid domain at different velocities. It was noticed that the drop in pressure for the D5 (Serpentine design) was high compared to the other design that was aimed at using OPCF material. Fig. 12 shows the effect on pressure drop as the specific fluid inlet velocities is varied in the range 1 m/s – 12 m/s for designs D1 – D5. It can be observed in Fig. 12, that D4 shows a very low-pressure drop, with a maximum of 20 Pa at a flow velocity of 12 m/s. The inset in Fig. 12 shows the pressure drop for a serpentine flow channel at a range of flow velocity 1 – 12 m/s, where the pressure drop is very high even at low flow velocities. In contrast to the traditional flow channels, the use of OPCF material shows better performance characteristics. Table 2 shows the boundary conditions that were used to run the optimisation of the flow plate.

384 Table 2 – Boundary conditions used in the simulation of the flow plates using Velocity

Meshing Properties		**Boundary Conditions**		**Solution Parameters**	
Mesher	ANSYS meshing	Model	OPCF	Solver	CFX
Mesh	Proximity and Curvature	Viscous model	Laminar	Solver type	Pressure based
Relevance	Fine	Fluid	Hydrogen	Scheme	Simple
Size function	Fixed	Solid	Aluminium	Gradient	Least Square Cells
Smoothing	Fine	Temperature	288 K	Discretisation pressure	Standard
Transition	Slow	Velocities	1, 3, 6, 9, 12 ms^{-1}	Momentum	Second order
Elements	250000 - 310000	Pressure Outlet	0	Porosity	0.90

385385

386 To obtain a comparison on the pressure drop in porous media, and to draw a contrast to the
387 simulation results obtained by ANSYS, the proposed mathematical models were analysed using
388 the values as shown in Table 3. Fig. 13 shows the pressure drop related to the different
389 mathematical models and the simulation result for design D4 from ANSYS. It is found that for the
390 same porosity $\zeta = 0.936$ and pore diameter, $d_p = 3.068\text{mm}$, the Darcy model, has the lowest
391 pressure drop which follows a similar trend to that of the pressure drop for design D4.

392392

393 Table 3: Parameter values used in the mathematical models

Parameters	***Values***	***Reference***
ζ	0.936	[49]
v	1.838×10^{-5} (kg/s m)	[49]
ε	4	[48]
d_p	3.068 (mm)	[7]
τ	1.308	[49]
ρ	1.184 ($kg/m^{3)}$	[49]
d_L	0.35 (mm)	[48]
α	0.4	[48]
L	5 (mm)	-

394394

395 Using the established result, that the Darcy model fits well with the ANSYS model simulation for
396 design D4, further analysis on the mathematical model is therefore performed. The Darcy model
397 in equation (2) relates to the pressure drop as a function of the permeability and the fluid velocity.
398 The permeability as described in equation (3) relates to the pore diameter and the porosity.

399 Fig. 14 shows the effect of increasing pore diameter for a constant porosity, $\zeta = 0.93$. It is
400 observed that the permeability of the material exponentially increases while the C factor reduces
401 and approaches a constant value for higher pore diameter [39]. This suggests that the pressure drop
402 for high pore diameter would have a linear response with increasing flow velocity. This can be
403 observed in Fig. 15, where the effect of increasing pore diameter is shown with respect to the
404 increasing velocity and the pressure drop. Further analysis on the effect of increasing porosity

suggest that for higher porosity, the pressure drop is lower. This effect can be observed in Fig. 15 (b) for a pore diameter of 100 µm.

Further utilisation of the Darcy model is carried out by analysing the overall effect on pressure drop in a 3D surface plot where the effect of varying pore diameter, porosity, and the flow velocity is considered. This can be observed in Fig. 16 (a), where a higher pore diameter and higher porosity shows a low-pressure drop. There is, however, a trade-off with a low-pressure drop at higher pore diameter, which is the flow regime of the operating fuel cell. For a fully functional PEMFC, it has been established that the flow through the channel is laminar. The Reynolds Number ($R_e = \frac{\rho\sqrt{\gamma}V}{v}$) is a good measure of determining the flow in a channel, where, $R_e < 2300$ indicates a laminar flow and turbulent otherwise [59-60]. It is dependent on the flow velocity and the permeability (pore diameter and porosity) of the channel, assuming a constant viscosity and density. This key measure is analysed for varying porosity, pore diameter and flow velocity in Fig. 16 (b). It is observed that for a flow velocity above 6 m/s and pore diameter of greater than 2 mm, the flow in the channel would therefore be turbulent. This result indicate that in the design of OPCF channel for consideration in PEM fuel cells, with higher pore diameter to achieve a low-pressure drop, the flow velocity should be less than 6 m/s.

One clear way of analysing fuel cell performance is through the polarisation curve. It is expected that, due to a low-pressure drop, fuel cell performance to be better. Mathematical models that describe the polarisation curve has been extensively studied in the literature [38], however, the performance can also be measured using a linear approximation of the polarisation curve, as this works well for most fuel cells acting within their practical operating range [38]. In analysing such performance, the permeability of the flow channel is a key parameter, which depends on the pore

diameter and the porosity for porous media. A linear approximation of the polarisation curve is therefore developed which is dependent on the permeability of the channel as defined earlier in equations (12) and (13). Fig. 17 shows a linear approximation of the polarisation curve for both the porous medium and hollow (serpentine) channel. All of the terms in equation (13) are kept constant for both types of channels except the permeability, which changes with the type of channel, as defined in equations (3) and (4). Fig. 17 shows the effect of using porous channel on the current density and cell potential. The result for the porous channel was evaluated for a pore diameter of $d_p = 0.25\text{mm}$ and porosity, $\zeta = 0.90$, whereas for the hollow serpentine channel, the hydraulic diameter (calculated) $d_h = 0.5$ mm was taken. The calculated permeability of the hollow channel was 2.02×10^{-8} m^2 and for the porous channel was 2.53×10^{-8} m^2. It is observed in Fig. 17 that, due to a low-pressure drop because of the use of OPCF flow channel, the performance of the PEM fuel cell is greatly increased. Based on the analysis carried out it can be concluded that for a good performance of the PEM fuel cell using OPCF material, the permeability should be greater than the traditional flow channel.

TESTING OF FUEL CELL

The fuel cell was also experimentally validated by testing the performance of the serpentine flow plate design with that of an open pore cellular foam material used in the new design. Fig. 18 shows the assembly process used in building the fuel cell with the open pore cellular foam material. The grooves were cut using a CNC machine to create the position where the aluminium open pore cellular foam will be placed. After the OPCFM is put in position, the membrane electrode assembly obtained from fuel cell store was also carefully placed on the foam. The cathode housing was also

designed to have the foam as its flow channel. The fuel cell was carefully tightened and checked for leaks, as any loss of hydrogen gas will compromise the economic efficiency of the new PEMFC design. Once checks showed the fuel cell was well sealed, it was then placed in the experimental set up as shown in Fig 19 and Fig.

The results obtained after using the open pore cellular foam material shown in Fig. 21 indicated that the fuel cell performance improved appreciably compared to the serpentine design and this also validated the results obtained computationally in ANSYS. It must be noted that the hydrogen was passed through a humidification chamber to keep the membrane moist to aid in good electro osmotic drag and back diffusion for both experiments. All other parameters, like cell operating temperature and pressure, were kept constant for both experiments. When the pressure drop through the bipolar plate between the inlet and outlet is high, more pumping power will be needed to overcome this, hence reducing the net performance of the fuel cell. The more gas is introduced to the catalyst layer, the more electrons are released hence the reason for the high performance of the fuel cell when the open pore cellular foam was used.

CONCLUSION

The general performance of a fuel cell depends highly on the pressure drop as well as the velocity of the gas as it flows through the fluid domain. High drop in pressure indicates that the flow of gas to the reactive site would be low. Therefore, the rate at which electrons will be released due to the electrochemical reaction will be lower, leading to a lower current produced. The work also identified that the design of the flow plate affects the water management of the fuel cell. Having a design where there are dead zones implies that not all portions (surface) of the MEA will be utilised during the electrochemical reaction. The orientations of the inlet and outlet also played a key role in determining the efficiency of the fuel cell. The drop in pressure of the foam was only subject to

the pores of the foam while that of the serpentine design experienced pressure drop in each arm of the flow channel. It explains the high-pressure drop for the serpentine flow plate design. The work finally concluded that, in comparison to the serpentine flow design, the open pore cellular foam material was a suitable option for a fuel cell with a minimum pressure drop of 22.5 Pa as compared to 10,000 Pa with the serpentine design at a velocity of 12 m/s.

REFERENCES

1. Tabbi Wilberforce, A. Alaswad, A. Palumbo, A. G. Olabi. Advances in stationary and portable fuel cell applications. International Journal of Hydrogen Energy 41(37) March 2016.
2. Tabbi Wilberforce, Ahmed Al Makky, A. Baroutaji, Rubal Sambi, A.G. Olabi. Computational Fluid Dynamic Simulation and modelling (CFX) of Flow Plate in PEM fuel cell using Aluminum Open Pore Cellular Foam Material. Power and Energy Conference (TPEC), IEEE, Texas. 2017. DOI: 10.1109/TPEC.2017.7868285
3. Tabbi Wilberforce, Ahmed Al Makky, A. Baroutaji, Rubal Sambi, A.G. Olabi Optimisation of bipolar plate through computational fluid dynamics simulation and modelling using nickle open pore cellular foam material. International conference on reneable energies and power quality (ICREPQ'17), ISSN 2171-038X, No 15 April 2017
4. Tabbi Wilberforce, A. Alaswad, J. Mooney,A.G.Olabi.Hydrogen Production for Solar Energy Storage. A Proposed Design Investigation.Proceedings of the 8th International Conference on sustainable Energy and Environmental Protection. ISBN: 978-1-903978-52-8

5. Baroutaji, A., Carton, J, G., Stoke, J., Olabi, A, G., 2014. Design and Development of Proton Exchange Membrane Fuel cell using the Open Pore Cellular Foam as flow plate material. Journal of Energy Challenges and Mechanics. Volume 1 (2014) issue 3.
6. Mikkola, M., 2001. Experimental studied on Polymer Electrolyte Membrane fuel cells stacks. Helsinki University of Technology, Department of Engineering Physics and Mathematics, Masters Thesis.
7. Carton, J. G., Olabi, A. G. Representative model and flow characteristics of open pore cellular foam and potential use in proton exchange membrane fuel cells. International Journal Of Hydrogen Energy 40 (2015) 5726 – 5738.
8. T. Wilberforce, Z. El-Hassan, F.N. Khatib, A. Al Makyy, A. Baroutaji, J. G. Carton and A. G. Olabi, Modelling and Simulation of Proton Exchange Membrane Fuel cell with Serpentine bipolar plate using MATLAB, International journal of hydrogen, 2017. DOI: 10.1016/j.ijhydene.2017.06.091.
9. J. G. Carton, V. Lawlor, A. G. Olabi, C. Hochenauer and G. Zauner, "Water droplet accumulation and motion in PEM fuel cell mini-channels", Energy, 39 (1), pp 63-73, 2012
10. Olabi AG. The 3rd international conference on sustainable energy and environmental protection SEEP 2009 the guest editor's introduction. Energy 2010;35:4508-9
11. V. Lawlor, S.Griesser, G.Buchinger, A.G.Olabi, S. Cordiner and D. Meissner, "Review of the micro-tubular solid oxide fuel cell: Part I. Stack design issues and research activities", J.Power Sources,193 (2),pp 387-399, 2009.
12. S. K. Dong, B. T. Yun and D. K. Lee, "Design and numerical study for l kW tubular SOFC APU system", Anonymous Fuel Cell Seminar, San Antonio; TX; United states: Electrochemical Society, Inc, October, pp- 701-706, 2007.

13. Tabbi Wilberforce, Zaki, El-Hassan, F.N. Khatib, A. Al Makyy, A. Baroutaji, J. G. Carton and A. G. Olabi. Developments of electric cars and fuel cell hydrogen electric cars. DOI: 10.1016/j.ijhydene.2017.07.054

14. Cook B. Introduction to fuel cells and hydrogen technology. Eng. Sci. Educ. J. 2002; 11(6): 205 – 16.

15. Superamaniam S. Fuel Cells: from fundamentals to applications. New York: Springer Science & Business Media: 2006.

16. Tsuchiya H, Kobayashi, O. Mass production of PEM fuel cell by learning curve. International Journal on Hydrogen Energy 2004; 29:985 – 90.

17. Chang HP, Chou CL, Chen Ys, Hou Ti, Weng BJ. The design and cost analysis of a portable PEMFC UPS system. International Journal on Hydrogen Energy 2007; 32:316 – 22.

18. Afsari E, Jazayeri SA. Effects of the cell thermal behavior and water phase change on a proton exchange membrane fuel cell performance. Energy Convers Manage 2010; 51: 655 – 62

19. A. D. Le and B. Zhou “A generalized numerical model for liquid water in a proton exchange membrane fuel cell with interdigitated design”, J.Power Sources ,193 (2), pp 665683,2009.

20. A. Kazim, H. T. Liu and P. Forges, “Modelling of performance of PEM fuel cells with conventional and interdigitated flow fields”, J.Appl.Electrochem, 29 (12), pp 1409-1416,1999.

21. J.P Kloess, X. Wang, J. Liu, Z. Shi and L. Guessous, “Investigation of bio-inspired flow channel designs for bipolar plates in proton exchange membrane fuel cells”, J.Power Sources, 188(1), pp 132-140, 2009.
22. Yoon YG, Lee WY, Park GG, Yang TH, Kim CS. Effects of channel and rib widths of flow field plates on the performance of a PEMFC. International Journal Hydrogen Energy 2005; 30:1363 – 6
23. Wang XD, Yan WM, Duan YY, Weng FB, Jung GB, Lee CY. Numerical study on channel size effect for proton exchange membrane fuel cell with serpentine flow field. Energy convers Manage 2010; 51:959 – 68.
24. Su A, Weng FB, Hsu CY, Cheng YM. Studies on flooding in PEM fuel cell cathode channels. International Journal Hydrogen Energy 2006; 31:1031 – 9.
25. Venkatraman M, Shimpalee S, Van Zee JW, Moon SI, Extrand CW. Estimates of pressure gradients in PEMFC gas channels due to blockage by static liquid drops, International Journal Hydrogen Energy 2009;34:5522 – 8.
26. Zhang HF, Pei PC, Yuan X. The conception of in – plate adverse – flow field for a proton exchange membrane fuel cell. International Journal Hydrogen Energy 2010; 35:9124 – 33.
27. Yazdi MZ, Kalbasi M. A novel analytical analysis of PEM fuel cell. Energy convers Manage 2010; 51:241 – 6.
28. Yan WM, Liu HC, Soong CY, Chen F, Cheng CH. Numerical study on cell performance and local transport phenomena of PEM fuel cells with novel flow field designs. Journal Power Sources 2006; 161:907 – 19.

562 29. Wang XD, Duan YY, Yan WM, Lee DJ, Su A, Chi PH. Channel aspect ratio effect for
563 proton exchange membrane fuel cell with serpentine flow field: role of sub – rib
564 convection. Journal Power Sources 2009; 193: 684 – 90.
565 30. A.P. Manso, F. F. Marzo, J. Barranco, X. Garikano, and M. Garmendia. Mujika, “Influence
566 of geometric parameters of the flow fields on the performance of a PEM fuel cell. A
567 review”, International Journal of Hydrogen Energy, 37 (20), pp 15256-15287, 2012.
568 31. Tseng, Chung-Jen, *et al.* "A PEM fuel cell with metal foam as flow distributor."Energy
569 Conversion and Management 62 (2012): 14-21.
570 32. C.J. Tsang, B.T. Tsai, Z.S. Liu, T.C. Cheng, W.C. Chang and S.K. Lo,”Effects of flow
571 field design on the performance of a PEM fuel cell with metal foam as the flow distributor”,
572 International Journal of Hydrogen Energy, 37 (17), pp 13060-13066, 2012.
573 33. A. Kumar and R.G. Reddy, “Materials and design development for bipolar/end plates in
574 fuel cells”, J Power Sources, 129 (1), pp 62-67, 2004.
575 34. A. Kumar, R.G. Reddy, “Modeling of polymer electrolyte membrane fuel cell with metal
576 foam in the flow-field of the bipolar/end plates”, J Power Sources, 114 (1),pp 54-62, 2003.
577 35. Maricle DL, Nagle DC. Carbon foam fuel cell components. US Patent 4,125,676; 1978.
578 http://www.virginia.edu/ms/research/wadley/Documents/Publications/Titanium_Matrix_
579 Composite_Lattice_Structure.pdf [Accessed: 16/10/2016]
580 36. C.J. Tsang, B.T. Tsai, Z.S. Liu, T.C. Cheng, W.C. Chang and S.K. Lo,”Effects of flow
581 field design on the performance of a PEM fuel cell with metal foam as the flow distributor”,
582 International Journal of Hydrogen Energy, 37 (17), pp 13060-13066, 2012
583 37. Kumar A, Reddy RG. Materials and design development for bipolar/end plates in fuel cells.
584 J Power Sources 2004; 129:62 – 7.

585 38. B. Ramos-Alvarado, A. Hernandez-Guerrero, F. Elizalde-Blancas and M.W.
586 Ellis,“Constructal flow distributor as a bipolar plate for proton exchange membrane fuel
587 cells”, International Journal of Hydrogen Energy, 36 (20), pp 1296512976, 2011.
588
589 39. Wang, Y. Porous-Media Flow Fields for Polymer Electrolyte Fuel cells. Journal of the
590 Electrochemical Society. 156(10) B1124 – b1133(2009)
591 40. Mathias, M, Roth, J, Fleming and Lernert W. Handbook of fuel cells: Fundamentals,
592 Technologies and Applications. Vielstich W., Gasteiger H, Lamm Editors, Vol 3, John
593 Wiley & Sons, New York (2003).
594 41. Medraj M, Baril, E, Loya V. The effect of microstructure on the permeability of metallic
595 foam. J Mater Sci (2007) 42:4372-4383
596 42. Lage JL(1998) In: Ingham BD, Pop I (eds) Transport phenomena in porous media. Pp 1-
597 30.
598 43. Gerbaux O, Buyens F, Mourzenko VV, Memponteil A, Vabre A, Thovert J-, *et al.*
599 Transport properties of real metallic foams. J Colloid Interface Sci 2010 2/1;342(1):155-
600 65
601 44. Zahi I, Rossi C, Faucheux V. Micro PEM fuel cell current collector design and optimization
602 with CFD 3D modeling. Int J Hydrogen Energy 2011 11;36(22):14562-72.
603 45. Kim TH, Lee W, Jeong JH. Thermo-fluidic characteristics of open cell metal foam as an
604 anodes for DCFC, part I: head loss open cell metal foam as an anodes for DCFC, part I:
605 head loss 2014;39(23):12369-76

606 46. Wilson L, Narasimhan A, Venkateshan SP. Permeability and form coefficient
607 measurement of porous inserts with non darcy model using non-plug flow experiments. J
608 Fluids Eng Trans ASME 2006;128(3):638-42
609 47. Dukhan N. Correlations for the pressure drop for flow through metal foam. Exp Fluids
610 2006 10;41(4):665-72.
611 48. Ashby MF, Evans AG, Fleck NA, Gibson LJ, Hutchinson JW, Wadley HNG. Metal foams:
612 a design guide. 1st ed. Massachusetts: Butterworth-Heinemann; 2000.
613 49. Du Plessis P, Montillet A, Comiti J, Legrand J. Pressure drop prediction for flow through
614 high porosity metallic foams. Chem Eng Sci 1994;49(21):3545-53.
615
616 50. Kumar A, Reddy RG. Modelling of Polymer electrolyte membrane fuel cell with metal
617 foam in the flow field of the bipolar/ end plates. J Power Sources 2003; 114: 54 – 62.
618 51. H. Liu and P. Li, “Even distribution/dividing of singlephase fluids by symmetric
619 bifurcation of flow channels” International Journal of Heat and Fluid Flow, 40, pp 165-
620 179, 2013.
621 52. H. Liu, P. Li and J.V. Lew,”CFD study on flow distribution uniformity in fuel distributors
622 having multiple structural bifurcations of flow channels”, International Journal of
623 Hydrogen Energy, 35 (17), pp 9186-9198, 2010
624 53. G.M. Imbrioscia and H.J. Fasoli, “Simulation and study of proposed modifications over
625 straight-parallel flow field design”, International Journal of Hydrogen Energy, 39 (16), pp
626 8861-8867 (2014).

54. A. Kumar and G.R. Reddy, “Effect of channel dimensions and shape in the flow-field distributor on the performance of polymer electrolyte membrane fuel cells”, Journal of Power Sources, 113 (1), pp 11-18, 2003.
55. E. Hontanon, M. J. Escudero, C. Bautista, P. L. GarcıaYbarra, and L. Daza, “Optimisation of flow-field in polymer electrolyte membrane fuel cells using computational fluid dynamics techniques." Journal of Power Sources, 86(1), pp 363368, 2000.
56. M. Mohammadi, G.N. Jovanovic and K.V. Sharp “Numerical study of flow uniformity and pressure characteristics within a microchannel array with triangular manifolds” Computers & Chemical Engineering, 52, pp 134144, 2013
57. A. Lozano, L. Valiño, F. Barreras, R. Mustata, “Fluid dynamics performance of different bipolar plates: Part II. Flow through the diffusion layer”, Journal of Power Sources, 179 (2), pp 711–722, 2008.
58. F. Barreras, A. Lozano, L. Valiño, C. Marín, A. Pascau, “Flow distribution in a bipolar plate of a proton exchange membrane fuel cell: experiments and numerical simulation studies”, Journal of Power Sources, 144 (1), pp 54–66, 2005.
59. Colleen, S. S., Designing & Building of fuel cell, 1st ed. ISBN 0-07-148977-0, McGraw – Hil, 2007.
60. Colleen, S. S., PEM Fuel Cell, Modelling, Simulation Using MATLAB. ISBN 978-0-12-374259-9, Academic Press, 2008.

Figure
Click here to download Figure: Figures - STE.docx

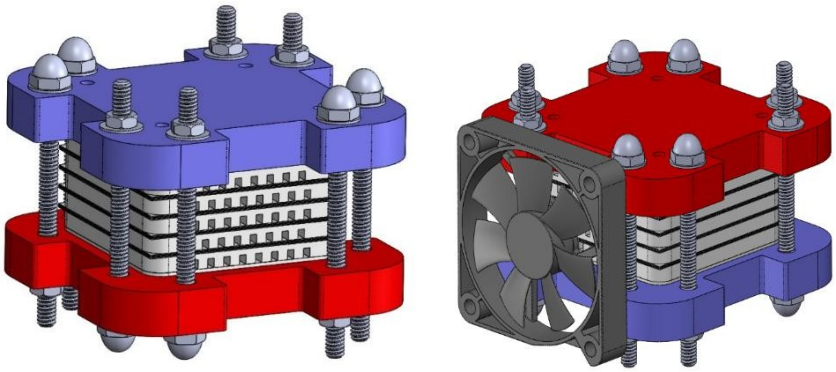

Fig. 1: Fuel cell with five (5) Stacks

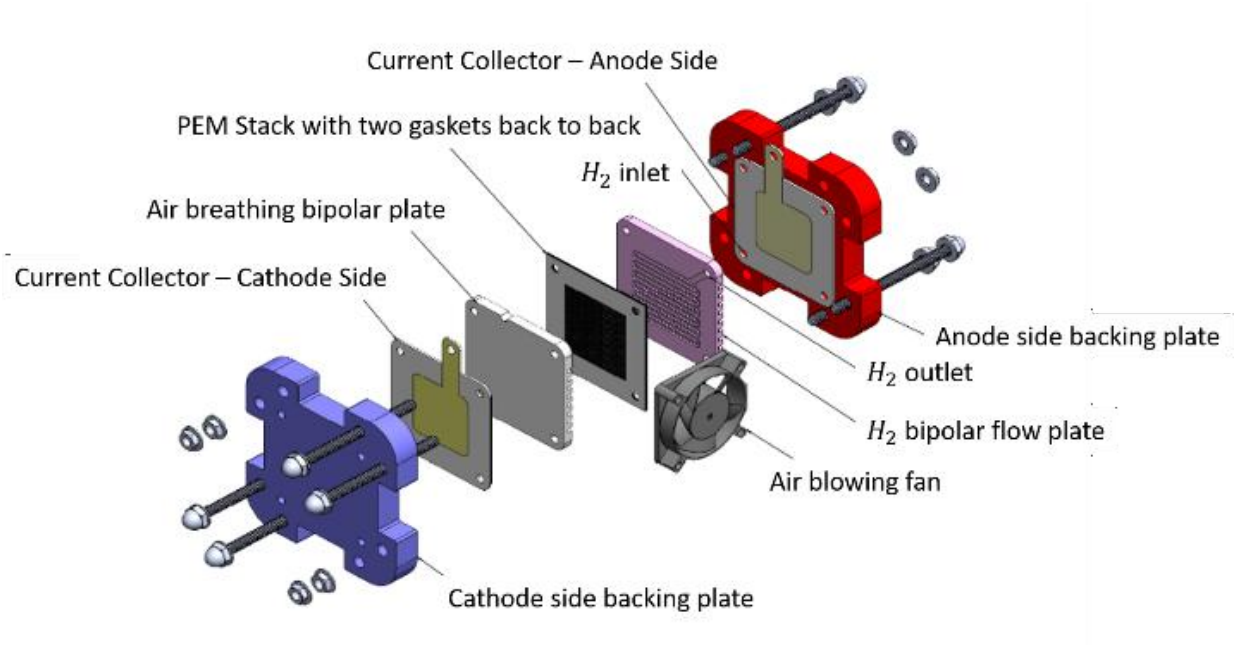

Fig. 2: Exploded view of a Proton Exchange Membrane fuel cell.

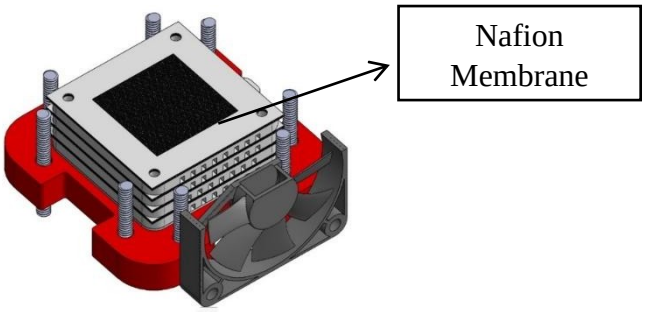

Fig. 3: Nafion Membrane Electrode assembly

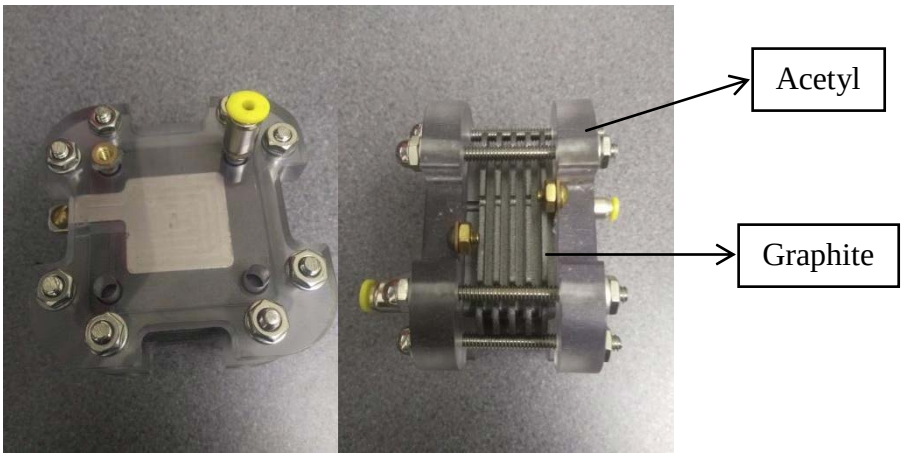

Fig. 4: PEM fuel cell with acetyl housing unit from obtained from fuel cell store.

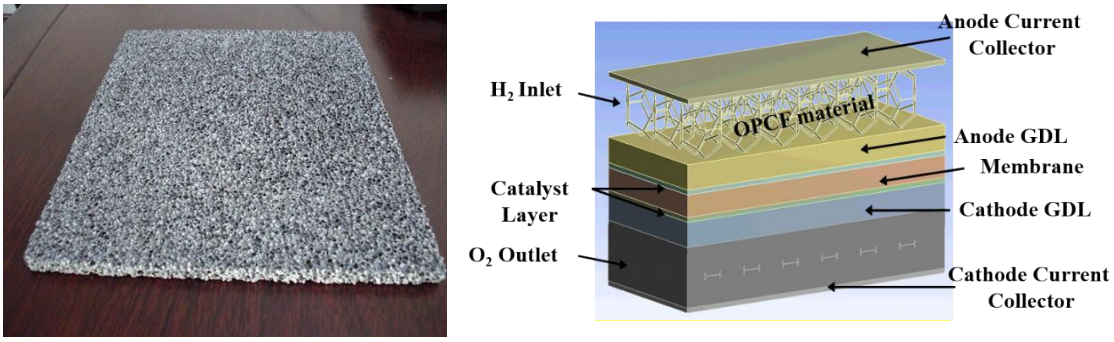

Fig. 5: OPCF material and the PEM Fuel cell schematic

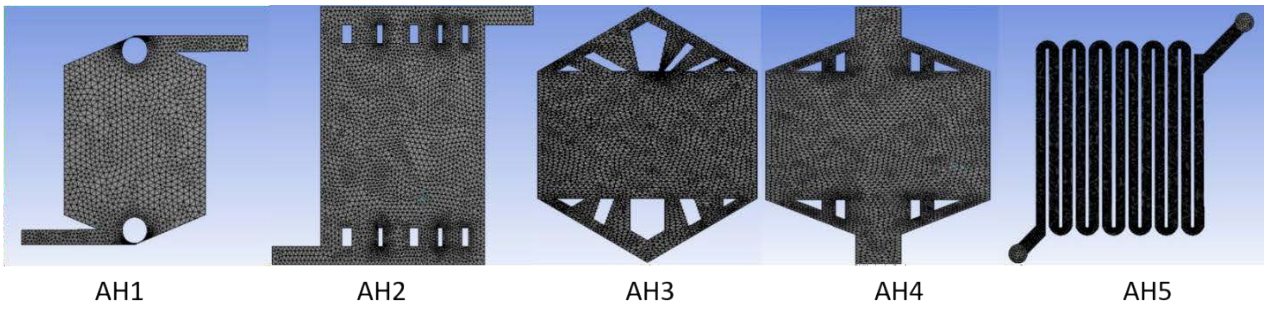

Fig. 6: The CFD model mesh using CFX.

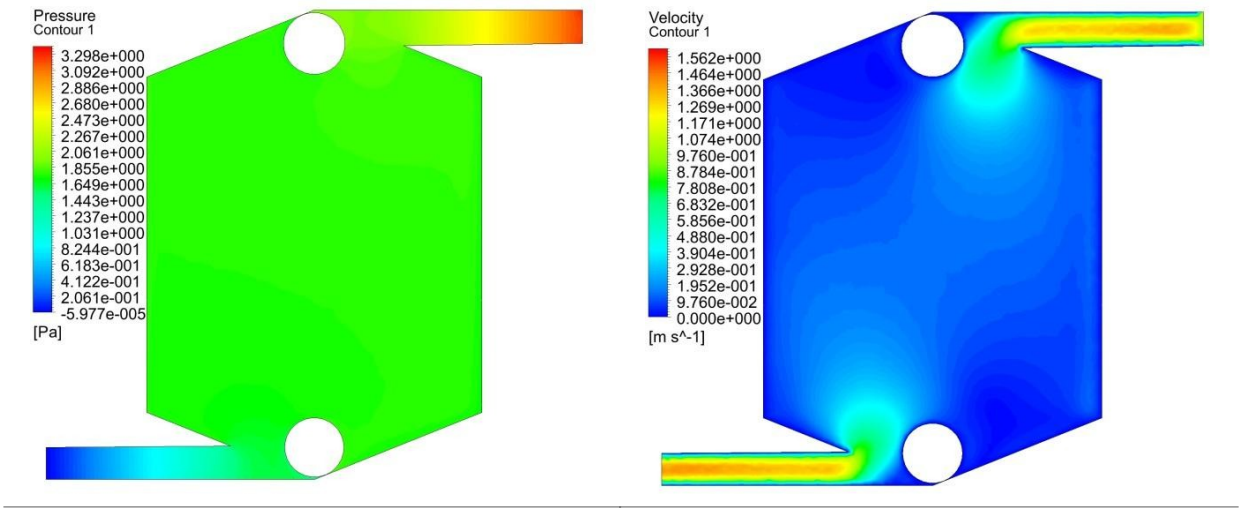

(a) (b)

Fig. 7: Fluid domain for flow channel D1: (a) - pressure profile (Pa), (b) - velocity profile(m/s)

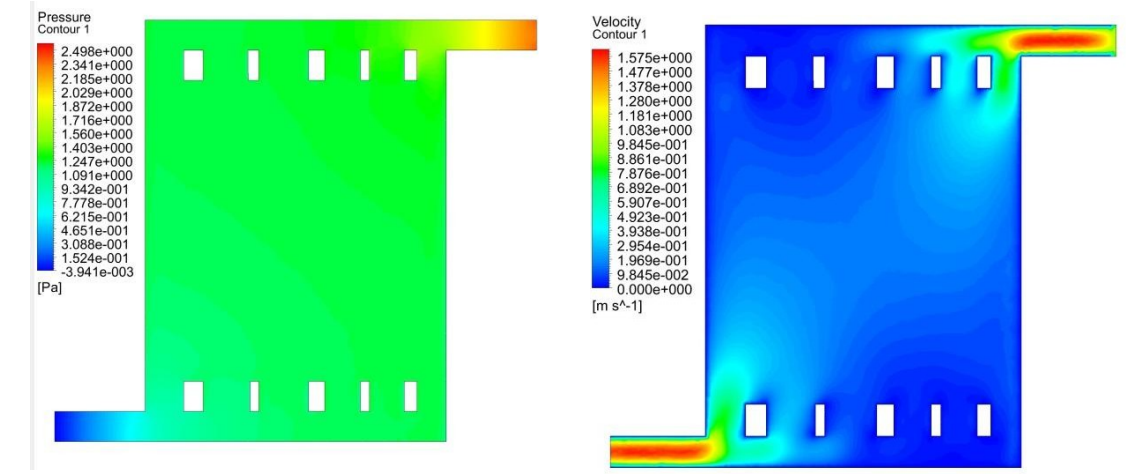

(a) (b)

Fig. 8: Fluid domain for flow channel D2: (a) - pressure profile (Pa), (b) - velocity profile(m/s)

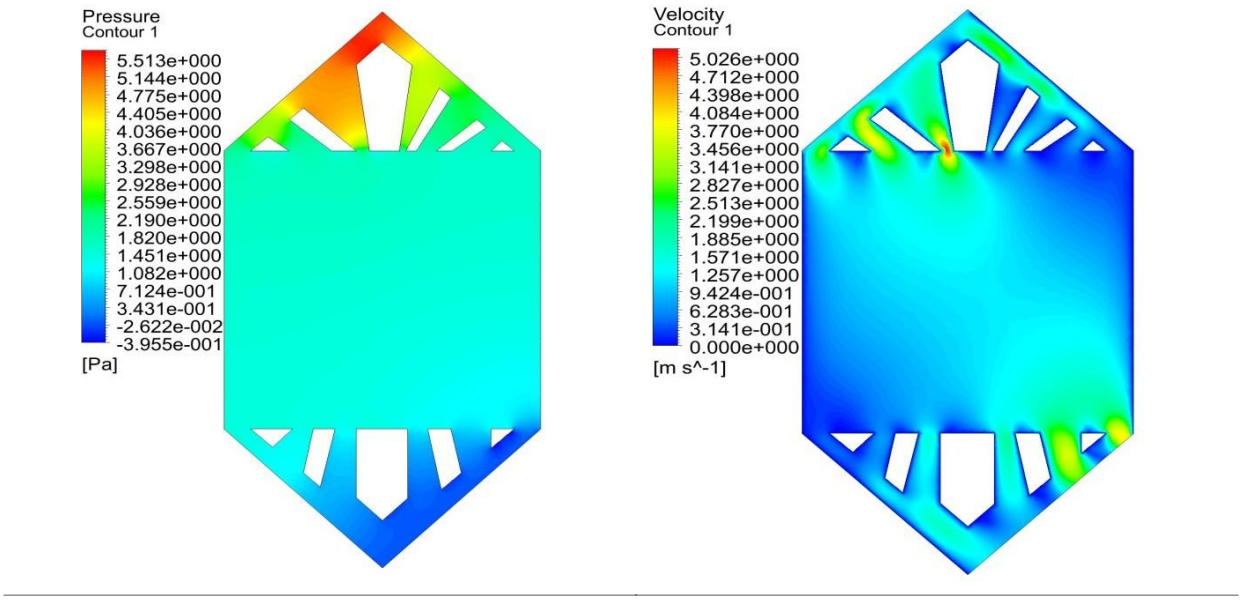

(a) (b)

Fig. 9: Fluid domain for flow channel D3: (a) - pressure profile (Pa), (b) - velocity profile(m/s)

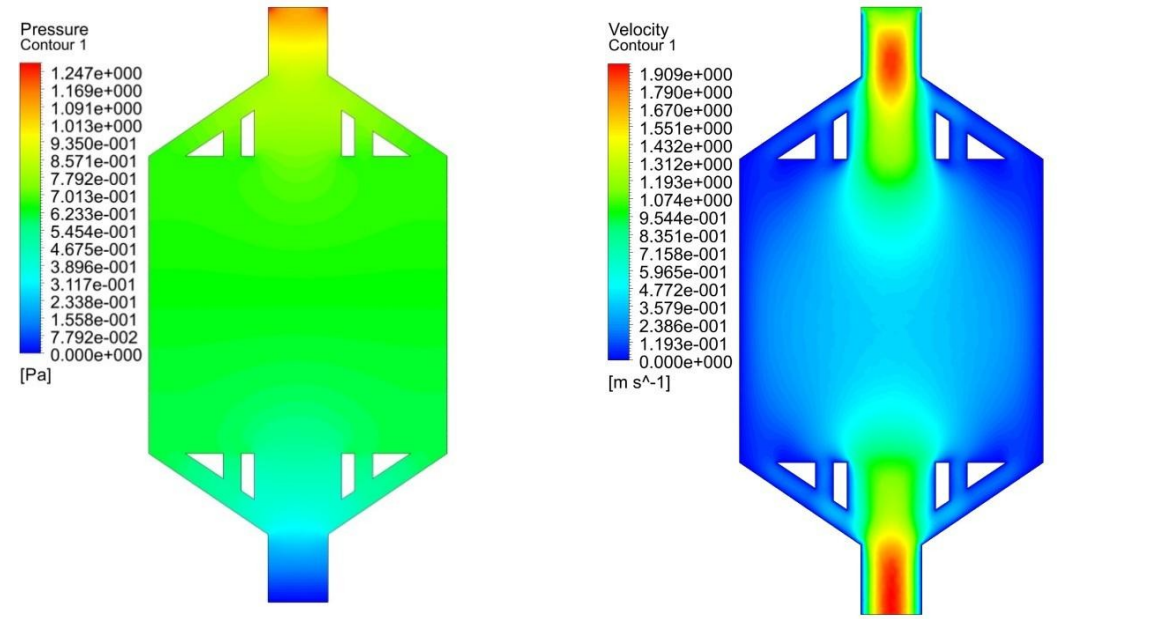

(a) (b)

Fig. 10: Fluid domain for flow channel D4: (a) - pressure profile (Pa), (b) - velocity profile(m/s)

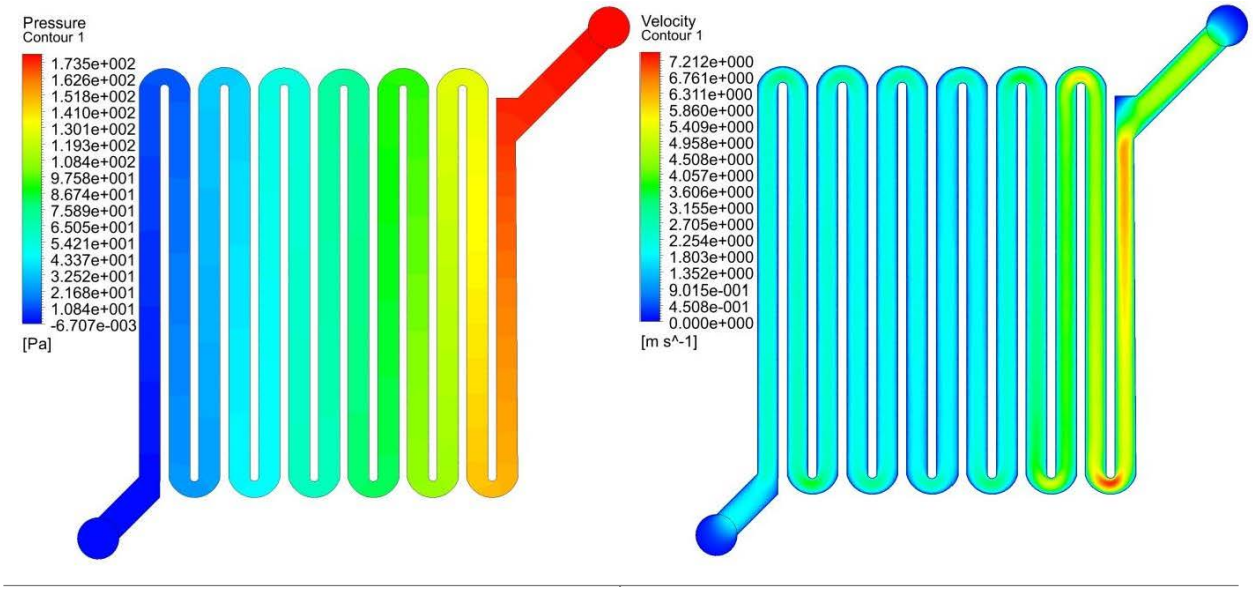

(a) (b)

Fig. 11: Fluid domain for flow channel D5: (a) - pressure profile (Pa), (b) - velocity profile(m/s)

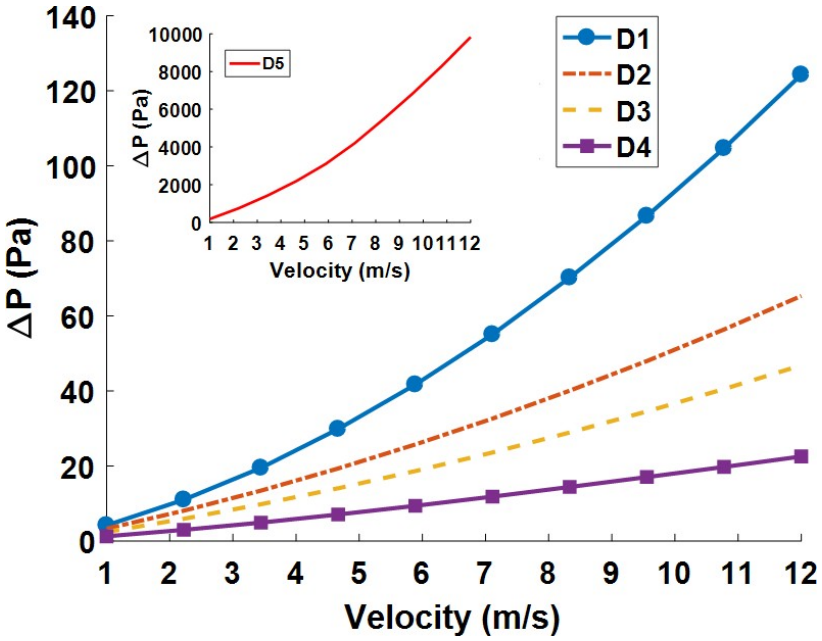

Fig. 12: Graph of velocity against pressure drop for flow channel designs D1 to D5.

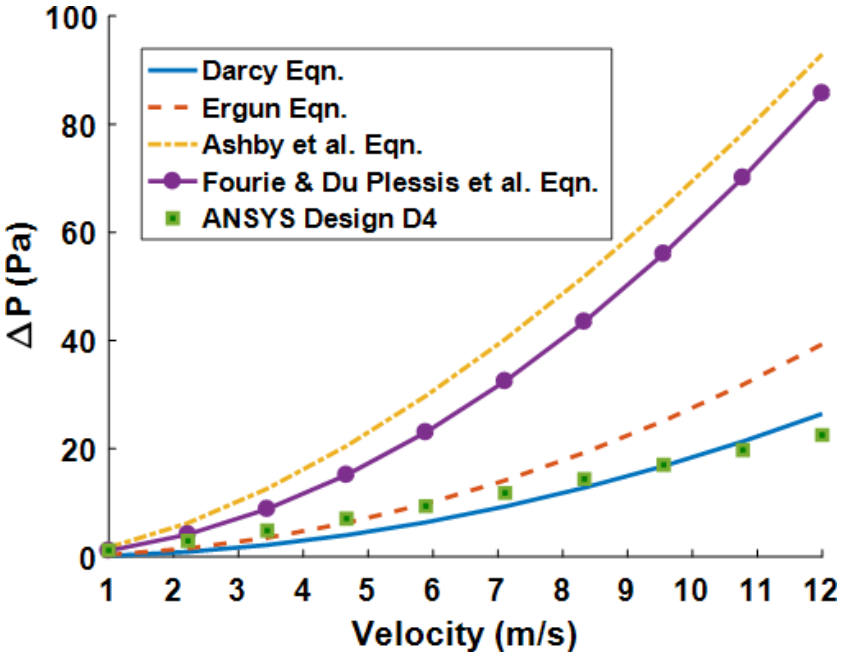

Fig. 13: Comparison of pressure drop using the different mathematical models and ANSYS simulation result for design D4.

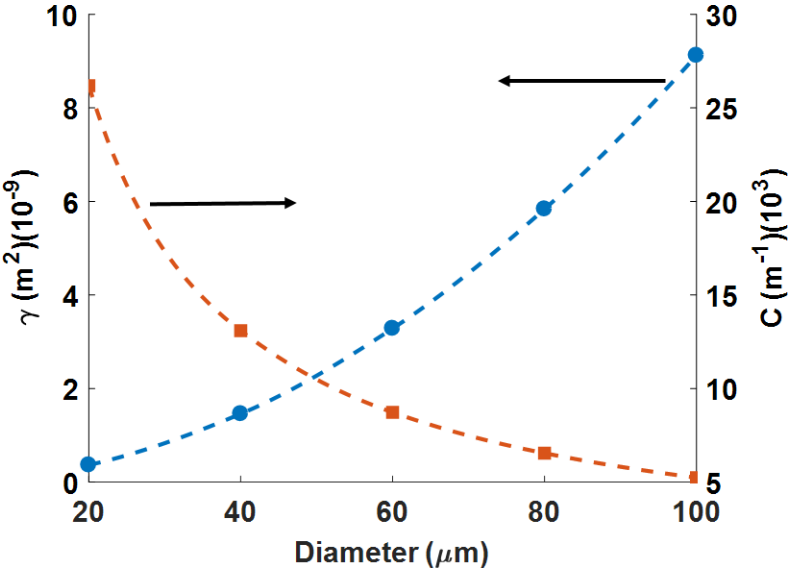

Fig. 14: Effect of increasing pore diameter on the permeability and factor C.

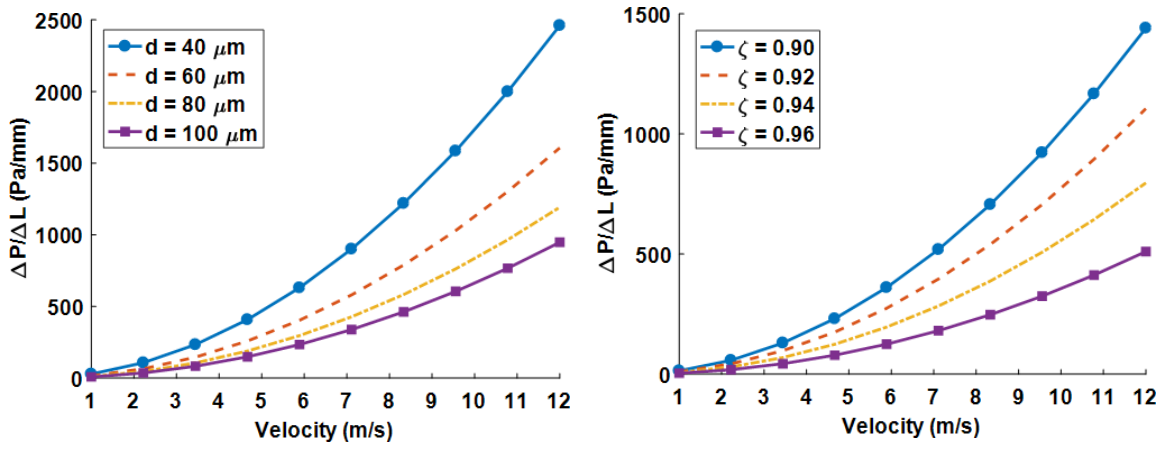

(a) (b)

Fig. 15: Effect of increasing velocity on pressure drop for (a) different pore diameter (b) different material porosity.

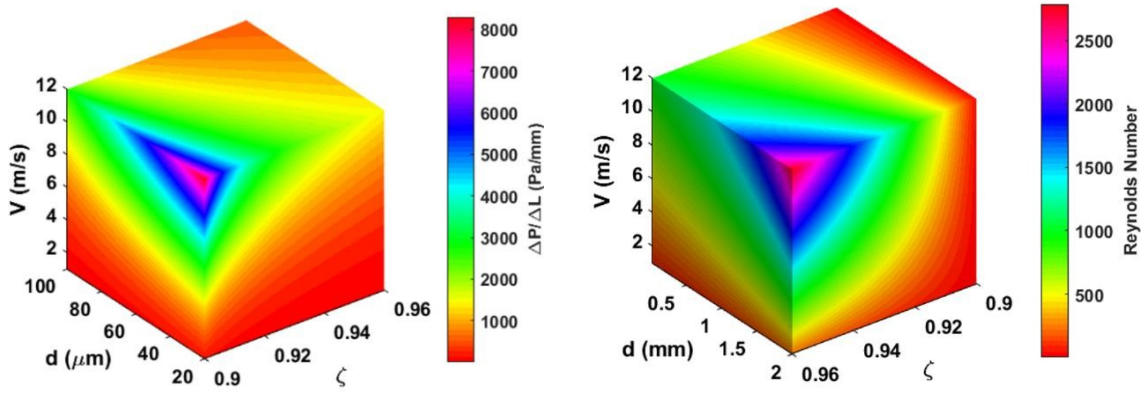

(a) (b)

Fig. 16: Surface plot at varying pore diameter, porosity and flow velocity for (a) Pressure drop (b) Reynolds Number

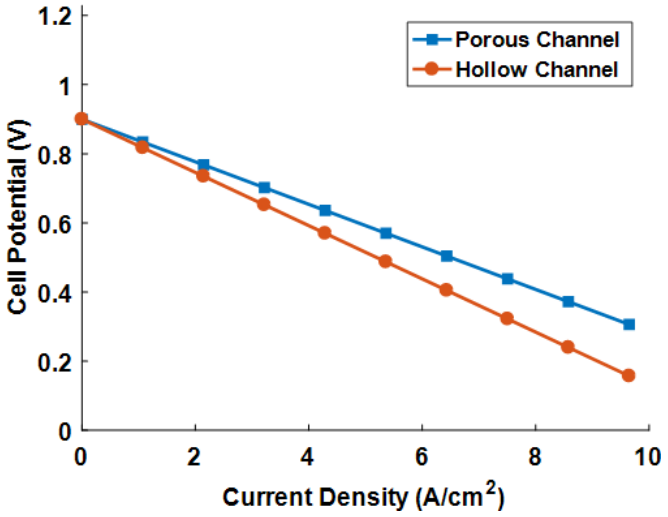

Fig. 17: Current density vs cell potential for the porous and hollow channel.

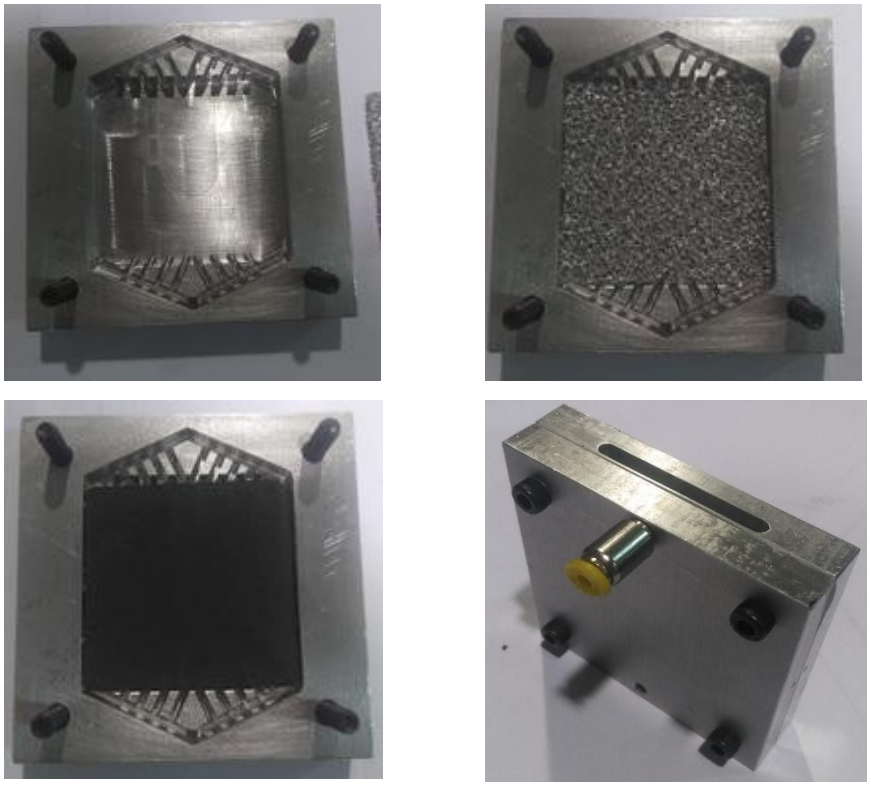

Fig. 18 Building of Open pore cellular foam material PEMFC.

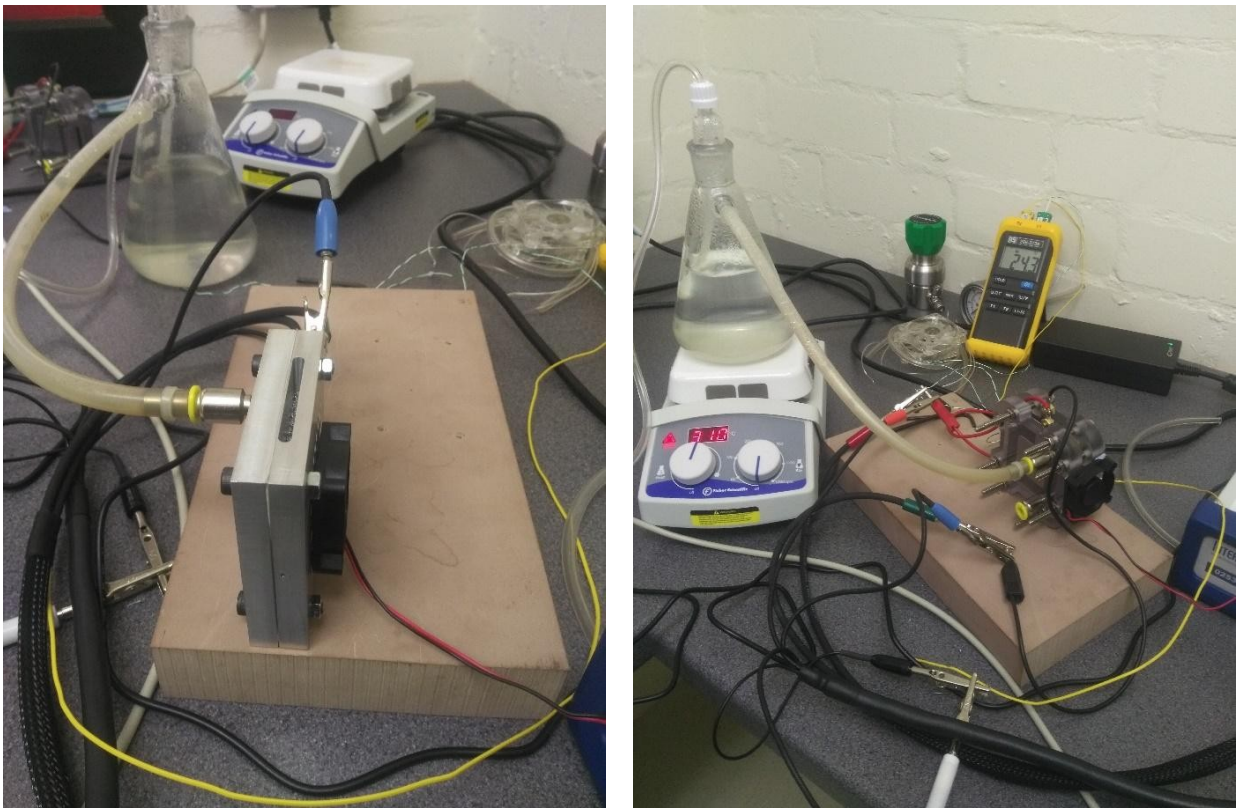

a) b)

Fig. 19: Experimental set up a) Open pore cellular foam material b) Serpentine flow field design

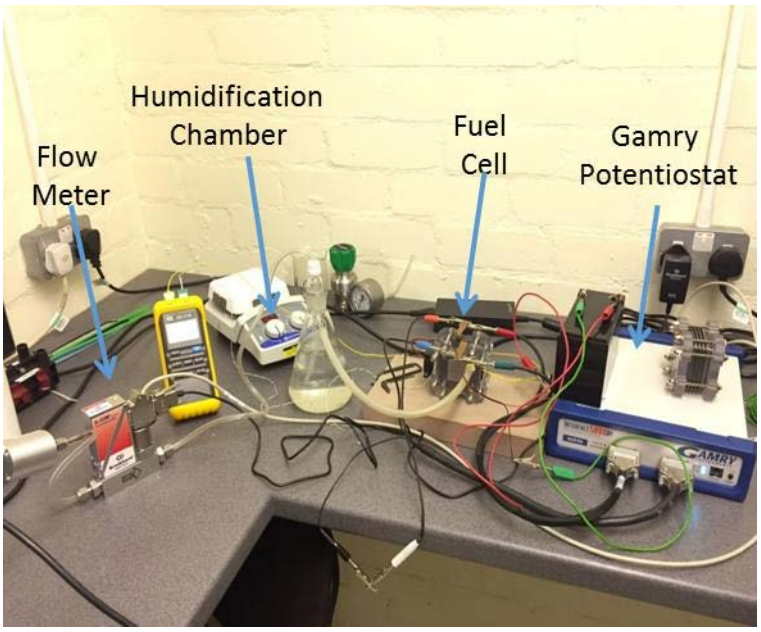

Fig 20: Experimental set up for the texting of the fuel cell

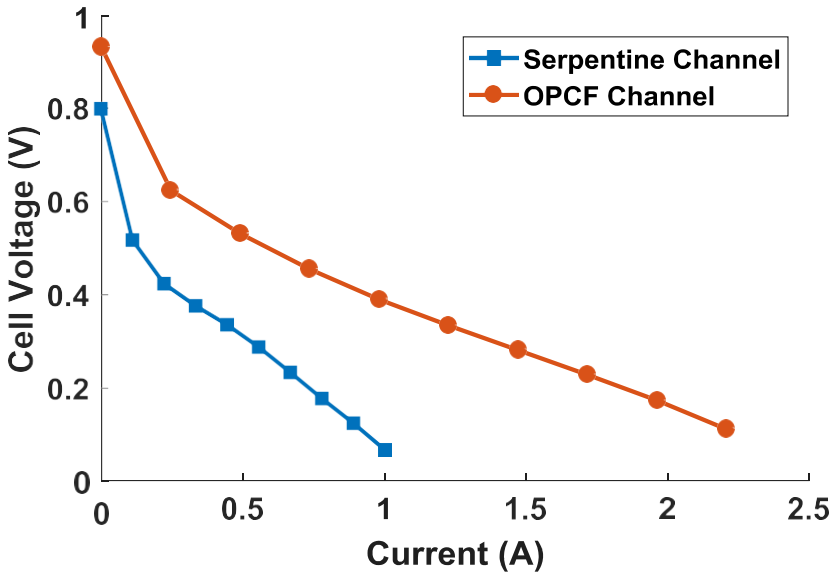

Fig. 21: Polarisation curve for the serpentine flow field and the open pore cellular foam material